

Application of Vector-Type Super Computer to Understanding Giant Earthquakes and Aftershocks on Subduction Plate Boundaries

Keisuke Ariyoshi, Toru Matsuzawa, Yasuo Yabe, Naoyuki Kato, Ryota Hino, Akira Hasegawa, and Yoshiyuki Kaneda

Abstract In order to know why megathrust earthquakes have occurred in subduction zones such as the 2011 off the Pacific Coast of Tohoku Earthquake in Japan, we reconsider previous numerical simulation results and try to apply them to actual fields such as the 2004 Sumatra-Andaman earthquake and large interplate aftershocks of the 2011 Tohoku Earthquake. From this study, we propose that one of the possible reasons of pre-seismic change of the 2011 Tohoku Earthquake might have been smaller for its magnitude because its fault was composed smaller ($M 7$ class) asperities including the off Miyagi earthquakes as occurred in 1978 and 2005. We also suggest that the next megathrust earthquake along Nankai Trough in southwest Japan may have detectable pre-seismic change because it is composed of three large ($M 8$ class) asperities in Tokai, Tonankai and Nankai region. Our trial numerical simulation results by using vector-type super computer show that Dense Oceanfloor Network System for Earthquakes and Tsunamis (DONET) may be useful to detect the pre-seismic change of a possible $M 9$ class coupled megathrust earthquake composed of Tokai, Tonankai, Nankai and Hyuga-nada asperities.

K. Ariyoshi (✉) · Y. Kaneda
Earthquake and Tsunami Research Project for Disaster Prevention, Japan Agency
for Marine-Earth Science and Technology, Yokohama 236-0001, Japan
e-mail: ariyoshi@jamstec.go.jp; kaneday@jamstec.go.jp

T. Matsuzawa · Y. Yabe · R. Hino · A. Hasegawa
Research Center for Prediction of Earthquakes and Volcanic Eruptions, Graduate School
of Science, Tohoku University
e-mail: matuzawa@aob.gp.tohoku.ac.jp; yabe@aob.gp.tohoku.ac.jp; hino@aob.gp.tohoku.ac.jp;
hasegawa@aob.gp.tohoku.ac.jp

N. Kato
Earthquake Research Institute, The University of Tokyo
e-mail: nkato@eri.u-tokyo.ac.jp

1 Introduction

1.1 Spatial Distribution of Mega-Thrust Earthquakes

In world history (Fig. 1), most of mega-thrust earthquakes have occurred near oceanic trenches accompanied with tsunami, especially around Japan. On the basis of asperity map [38] or spatial distribution of source area of historical earthquakes [37], faults of megathrust earthquakes are thought to be composed of multi-segment. For examples, the 2004 Sumatra Andaman Earthquake is thought to rupture from Sumatra segment through Nicobar segment to Andaman segment [19]. The 2011 off the Pacific Coast of Tohoku Earthquake is thought to be composed of three main ruptured zones off Miyagi, far off Miyagi, and off Ibaraki [13], which generates tremendous tsunami in Miyagi, Iwate and Fukushima prefectures. In this chapter, we refer to the phenomenon that nearby earthquakes occur after time-lag significantly shorter than recurrence interval as “coupled earthquakes”.

1.2 Modelling of Coupled Earthquakes

Ariyoshi et al. [1, 2] categorized the characteristics of the coupled earthquakes into two models: (i) Model of slip proportional to fault size, and (ii) Characteristic slip model. In the following sections, we review the two proposed model.

Figure 2 shows an example of model of slip proportional to fault size. For that slip amount (D) proportional to fault size has two types: “ L -model” proportional to fault length (L) [32], and “ W -model” proportional fault width (W) [28]. In case of proportional relation between W and L , both L -model and W -model are the same relation as similarity model with stress drop ($\Delta\sigma$) constant [14]. For coupled earthquakes, however, it is possible that the aspect ratio (L/W) of fault does not always keep constant as discussed later.

Figure 3 shows an example of characteristic slip model. Coupled earthquake keeps slip amount same as single earthquake. In other words, slip amount is independent of fault size (W and L) even if several earthquakes on the same fault occur simultaneously, which was observed in the North Anatolian fault [18] and the 1992 Landers earthquake [33].

1.3 Application to Actual Earthquakes

For inland earthquakes with lateral faults and high dip angle, the upper limitation of fault width tends to significantly lower than fault length [28]. This is probably because seismic slip decays abruptly in asthenosphere. It is thought that matured active faults often have deeper part of fault reaching asthenosphere (Fig. 4). This means that fault width cannot develop for deeper part any more, and keeps constant

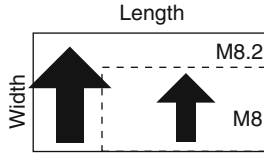


Fig. 2 Schematic illustration of “model of slip proportional to fault size” in case of $L = 2W$ [14]. Bold arrow size represents slip amount (D). This figure is revised from Ariyoshi and Kaneda [3]

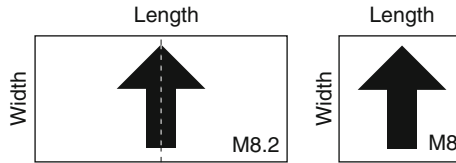


Fig. 3 Schematic illustration of characteristic slip model by comparing between coupled earthquake (left) and single earthquake (right). This figure is revised from Ariyoshi and Kaneda [3]

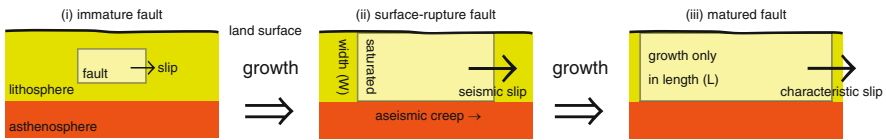


Fig. 4 Schematic illustration of fault growth process: (i) immature fault, (ii) fault with saturated width, and (iii) matured fault with the same slip amount as (ii). In case of “ W -model”, characteristic slip model is applicable between (ii) and (iii) because of failure of seismic slip to occur in asthenosphere. This figure is revised from Ariyoshi and Kaneda [3]

width in case of large earthquakes. Since keeping constant fault width makes constant slip amount for “ W -model”, “characteristic slip model” may be applied to matured active faults from the view of “ W -model” [9].

For trench-type megathrust earthquakes, the upper limitation of fault width may be high enough to avoid saturation because of low dip angle. For examples, fault geometry ($width \times length$) of the 2011 off the Pacific Coast of Tohoku Earthquake is thought to be 500×200 km [13], and sub-fault geometries of the 2004 Sumatra Andaman earthquake are 420×240 km for Sumatra segment, 325×170 km for Nicobar segment and 570×160 km for Andaman segment, respectively [19].

By treating the three sub-faults of the 2004 Sumatra Andaman earthquake as one giant fault, its aspect ratio does not keep constant as obeyed in the “model of slip proportional to fault size”. On the other hand, the “characteristic slip model” would not quantitatively explain 20 m of its maximum slip amount.

In this chapter, we discuss the validity of both the “model of slip proportional to fault size” and “characteristic slip model” in some cases on the basis of numerical simulations, revealing the unknown characteristics and give a road map for earthquake prediction.

2 Numerical Simulation Studies

The two proposed model: “characteristic slip” and “slip proportional to fault size” is investigated from numerical simulation studies done by Ariyoshi et al. [1] and Kato [15], respectively. In this section, we review their calculation method and results, comparing slip behaviors and detectability between them.

2.1 Method of Earthquake-Cycle Simulations

In order to focus specifically on the physical mechanisms of fault segment interaction, a planar plate interface is assumed in a homogeneous elastic half-space. The plate interface deeper than 103 km is assumed to slip at a constant rate of V_{pl} (relative velocity between the continental and oceanic plates) and the shallower part is divided into N cells. The slip for each cell is assumed to involve only a shear component in the dip direction and to obey a quasi-static equilibrium condition between the shear stress due to dislocation ($\tau_i^{dislocation}$) and frictional stress ($\tau_i^{friction}$). The stress is assumed to have both shear and normal components (σ_i) in the dip direction. The equations used in the simulation are as follows:

$$\tau_i^{dislocation}(t) = \sum_{j=1}^N K_{ij}(u_j(t) - V_{pl}t) - (G/2\beta) \frac{du_i}{dt}, \quad (1)$$

$$\sigma_i(t) = \sum_{j=1}^N L_{ij}(u_j(t) - V_{pl}t) + (\rho_r - \rho_w)gy, \quad (2)$$

$$\tau_i^{friction}(t) = \mu_i(t)\sigma_i(t), \quad (3)$$

$$\tau_i^{dislocation}(t) = \tau_i^{friction}(t), \quad (4)$$

Here the subscripts i and j denote the cell locations of an observation and a source, respectively. In Eqs. (1) and (2), K_{ij} and L_{ij} represent analytical Green’s functions due to slip $u_j(t)$ in the j th cell for the shear and normal stress on the i th cell, respectively [23, 26]. The term $(u_j(t) - V_{pl}t)$ implies that we consider stress generated only by the amount of slip relative to the long-term average plate convergence [31]. The last term in Eq. (1) represents seismic radiation damping [27], where G and β are rigidity and shear wave speed, respectively. The last term in Eq. (2) represents the static effective normal stress assuming hydrostatic pressure, where ρ_r and ρ_w are the densities of rock and water, g is gravity acceleration, and y is depth. Equations (3) and (4) represent the frictional stress and the quasi-static equilibrium condition, respectively. The friction coefficient μ in Eq. (3) is assumed to obey a rate-and-state-dependent friction law [8, 29] given by

$$\mu_i = \mu_0 + a_i \log\left(\frac{V_i(t)}{V_0}\right) + b_i \log\left(V_0 \frac{\theta_i(t)}{d_{ci}}\right), \quad (5)$$

$$\frac{d\theta_i(t)}{dt} = 1 - V_i(t) \frac{\theta_i(t)}{d_{ci}}, \quad (6)$$

where a and b are friction coefficient parameters, d_c is the characteristic slip distance associated with b , θ is a state variable for the plate interface, V is slip velocity ($= \frac{du_i(t)}{dt}$), and μ_0 is a reference friction coefficient defined at a constant reference slip velocity of V_0 . The friction coefficient converges to a steady state value of $\mu_i^{ss} = \mu_0 + (a_i - b_i) \log\left(\frac{V_i}{V_0}\right)$ when the slip velocity remains constant at V_i for a distance sufficiently longer than d_{ci} [29]. Therefore, μ_i^{ss} at velocity V_i is a function of $\gamma_i = (a_i - b_i)$, which represents frictional stability. If $\gamma_i > 0$, the slip is stable because frictional stress increases as the slip velocity increases, behaving like viscosity. If $\gamma_i < 0$, the slip is unstable and exhibits stick-slip behavior. The modeled spatial distributions of these frictional parameters are introduced in the next section. The six equations above are solved using the Runge–Kutta method with adaptive step-size control [25].

2.2 A Simulation of Characteristic Slip and Slip Proportional to Fault Size

In case of characteristic slip, Ariyoshi et al. [1] performed a simulation of Miyagi-oki earthquakes in a 2-D subduction plate boundary. Their simulation results show that pre- and post-seismic slip for following earthquakes of coupled earthquakes tend to be amplified significantly (about 2–4 times), while amplification of co-seismic slip is slightly (about 13–36%). These results suggest that following earthquakes of coupled earthquakes with characteristic slip is more detectable than single earthquakes with same magnitude.

In case of slip proportional to fault size, Kato [15] formulated two adjacent large asperities reproducing the 1968 Tokachi-oki earthquake (M_w 8.2) breaking both the asperities and the 1994 Sanriku-oki earthquake (M_w 7.8) breaking one characteristic asperity [21]. Ariyoshi et al. [2] pointed out that seismic slip of the 1968 earthquake is approximately twice of the 1994 earthquake, considering that the ratio of seismic moment is $8.2/7.8 = 0.4$ and the asperity area ratio is almost 2 because both asperity has nearly same area. On the other hand, Kato [15] showed the simulation result that pre-seismic slip amount for the 1968 earthquake is nearly the same as the 1994 earthquake. These results suggest that a triggering nearby earthquake in case of “model of slip proportional to fault size” largely affects only on co-seismic slip, not on pre-seismic slip.

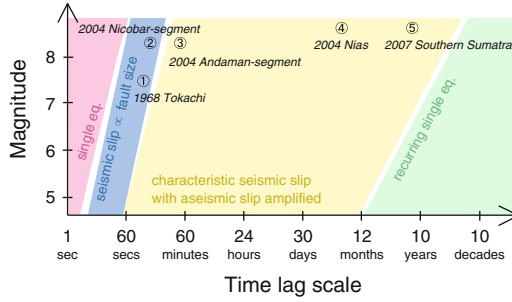


Fig. 5 A schematic relation between time lag, magnitude and slip model for the triggered earthquake of coupled earthquakes developed from Ariyoshi et al. [2]. Encircled numbers represent recently observed examples: (1) the 1968 Tokachi earthquake [21], (2) Nicobar segment of the 2004 Sumatra Andaman earthquake [19], (3) Andaman segment of the 2004 Sumatra Andaman earthquake [5, 19], (4) the 2004 Nias earthquake [6, 37], (5) the 2007 Southern Sumatra earthquake [17, 37]

2.3 Relation Between Characteristic Slip with Slip Proportional to Fault Size

Figure 5 shows a schematic relation between slip model and time lag of coupled earthquake on the basis of magnitude for the following (triggered) earthquake. As an example, we apply some coupled earthquakes regarding to the 2004 Sumatra Andaman earthquake into the relation in Fig. 5. Table 1 summarized slip components for the three sub-faults of the 2004 Sumatra earthquake which ruptured three seismogenic segments along trench—the Sumatra, Nicobar, and Andaman segments—and the average amount of co-seismic slip in each segment was roughly estimated at about $7m$, $5m$ and $<2m$, respectively [19]. The fault size factor of the coupled Nicobar and Sumatra segments relative to the Nicobar segment alone is about 2.35 (where the respective sizes (*trench* \times *dip direction*) of the Sumatra and Nicobar segments are $(420 \times 240) \text{ km}^2$ and $(325 \times 170) \text{ km}^2$, respectively, and $((420 + 325)\text{km} \times (240 + 170)\text{km}/(325 \text{ km} \times 170 \text{ km}))^{0.5} \sim 2.35$) and the co-seismic slip amount of single-event earthquakes rupturing the Nicobar segment is estimated to be $2.7 \pm 0.3 \text{ m}$ based on the 1881 earthquake [5].

This implies that the co-seismic slip amount of the Nicobar segment is approximately proportional to fault size and, therefore, the stress drop model is preferable in describing interaction between the Sumatra and Nicobar segments. On the other hand, the observed co-seismic slip amount for the Andaman portion of the rupture is roughly the same as in the 1941 Andaman earthquake ($2\text{--}3m$ [5]) and post-seismic slip is substantial ($\sim 5m$, [19]), meaning that the characteristic slip model is preferable to account for interaction between the Nicobar and Andaman segments.

The 2005 Nias earthquake adjacent to the Sumatra segment occurred about three months after the 2004 Sumatra Andaman earthquake and was followed by the 2007 Southern Sumatra earthquake [17, 37] easterly adjacent to the source region of the

Table 1 Summary of slip components for the three segments ruptured by the 2004 Sumatra earthquake. Transit time represents time elapsed from the origin time of the 2004 Sumatra earthquake. D_{seis} and D_{slow} represent slip amounts for co-seismic and aseismic (slow) component, respectively [19]. D_{single} represents coseismic slip amount for single event based on previous researches [5] for comparison [2]

Segment	D_{seis} (Transit time)	D_{slow} (Transit time)	D_{single}
Sumatra	7m (0–50 s)	Not resolved	Not known
Nicobar	5m (230–350 s)	5m (230–3,500+ s)	$2.7 \pm 0.3 m$
Andaman	<2m (350–600 s)	5m (600–3,500+ s)	2–3m

Nias earthquake. Both of their post-seismic slips were amplified in western part [12], which were the same as directions of after-slip (post-seismic slip) arrivals [17, 37]. On the 2005 Nias earthquake (M_w 8.6), its seismic magnitude was largely equal to the 1861 Nias earthquake (M 8.5) which occurred as single event, which is largely equal to the 2005. On the 2007 Southern Sumatra earthquake (M_w 8.5), its magnitude was neither as much as previous events occurred in 1833 (M 8.9) nor moment magnitude expected from slip deficit [17]. These results also imply that the 2005 Nias earthquake and the 2007 Southern Sumatra earthquake were applied to the “characteristic slip model”.

3 Discussion: A Question About the 2011 Tohoku Earthquake

Figure 6 shows asperity map of major trench-type megathrust earthquakes around Japan with spatial distribution of co-seismic slip for the 2011 off the Pacific Coast of Tohoku Earthquake. Focusing on the 2011 off the Pacific Coast of Tohoku Earthquake, we find that its source region covers some major asperities ($M7 \sim 8$) which overlap or neighbour each other. Unfortunately, it is well-known that pre-seismic change such as crustal deformation and seismicity has not been observed significantly. These observational results may suggest that the 2011 off the Pacific Coast of Tohoku Earthquake is composed of several asperities which behave as the “model of slip proportional to fault size” as mentioned above. In other words, pre-seismic change of the 2011 off the Pacific Coast of Tohoku Earthquake may be as small as $M7$ class earthquakes as observed for the 1968 Tokachi-oki earthquake [15]. In off Kanto and Boso, southward of the 2011 off the Pacific Coast of Tohoku Earthquake, there are several major source regions including the 1923 great Kanto earthquake ($M7.9$) and the 1953 off Boso peninsula earthquake ($M7.4$) which generated large tsunamis. Since both the earthquakes are far away from the source region of the 2011 off the Pacific Coast of Tohoku Earthquake, both the southward major earthquake may behave as the “characteristic slip model”. This suggests that their pre-seismic changes may be amplified so as to be detected by oceanfloor observations such as acoustic GPS [16] and/or repeating earthquakes[36].

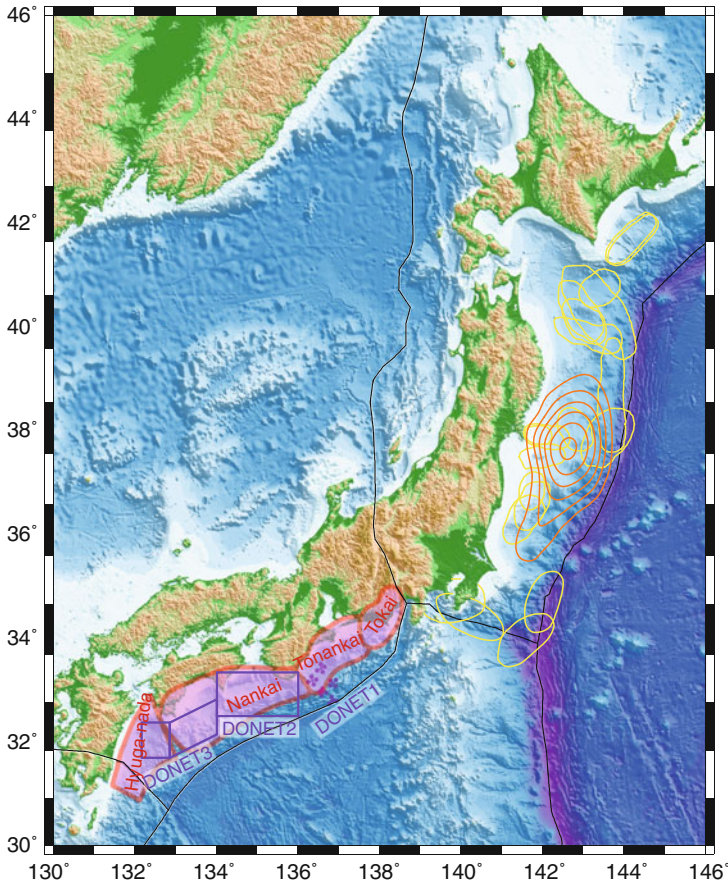


Fig. 6 Map of major asperities around Japan. *Black curves* are plate boundaries [24]. *Orange contours* represent co-seismic slip of the 2011 off the Pacific Coast of Tohoku Earthquake [11] as interval of 4 m. *Yellow ellipses* are the estimated source regions of past megathrust earthquakes (excluding outer-rise earthquakes) around the 2011 off the Pacific Coast of Tohoku Earthquake [34]. *Pink regions* from east to west along Nankai trough represent the seismogenic zones of Tokai, Tonankai, Nankai and Hyuganada earthquakes [35]. *Purple filled circles* and *open rectangle* regions represent observation points of DONET 1 and regions of DONET 2 and 3, respectively. This figure is modified from Ariyoshi and Kaneda [3]

Therefore, what we have to do is to develop:

- 3-D subduction plate model from geological surveys.
- Friction law based on rock laboratory experiments.
- Large-scale numerical simulations to combine above results.

These studies would determine the type of coupled earthquakes (slip proportional to fault size or characteristic slip) for major megathrust earthquakes including the 2011 Tohoku Earthquake.

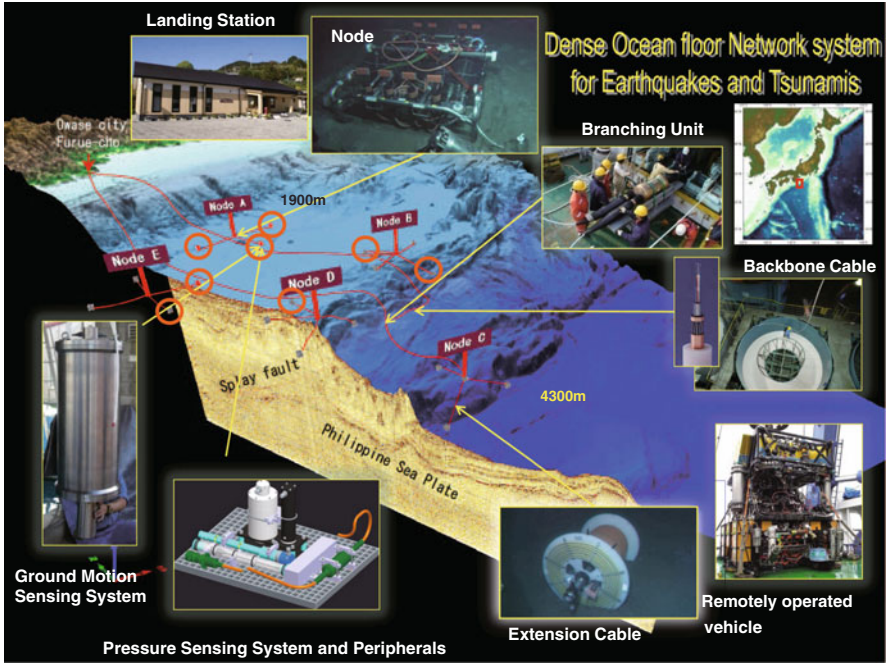


Fig. 7 An overview of Dense Oceanfloor Network System for Earthquakes and Tsunamis (DONET) in Tonankai region (DONET 1 in Fig. 8). This figure is modified from Ariyoshi and Kaneda [4]

4 Future Megathrust Earthquakes Around Japan

On the megathrust earthquakes along the Nankai Trough, it is thought that Tokai, Tonankai and Nankai earthquakes may occur in the near future and some researchers have pointed out that Hyuga-nada earthquake may be triggered by the $M9$ class coupled earthquakes composed of the three megathrust earthquakes [10]. However, size of asperities composing the possible $M9$ class coupled earthquakes along the Nankai Trough is significantly larger than that of the 2011 off the Pacific Coast of Tohoku Earthquake which may be composed of $M7$ class as shown in Fig. 6. This suggests that pre-seismic change of the possible $M9$ class coupled megathrust earthquakes along the Nankai Trough may be larger and is expected to be as large as the 1944 Tokai earthquake with detectable pre-seismic change reported by some researchers [20, 30]. Therefore, real-time monitoring of crustal deformation and seismicity is essential for us to detect the pre-seismic change in advance.

Figure 7 shows an overview of Dense Oceanfloor Network System for Earthquakes and Tsunamis (DONET) toward an anticipated Tonankai Earthquake. All of the twenty sets of preliminary interface have been installed just on July 31, 2011 and are to be prepared in consideration of the improvement of observation capability in the future.

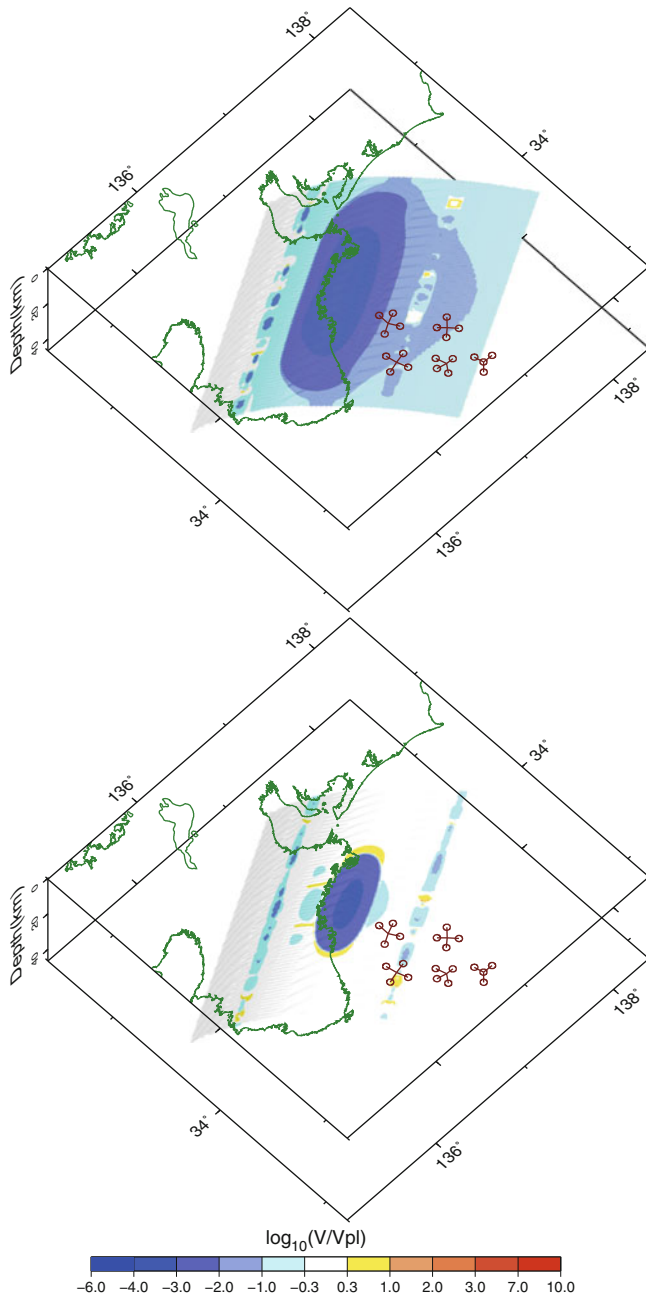


Fig. 8 Snapshots of slip velocity on the plate boundary about 20 years after the megathrust earthquake (*top*; interseismic period) and 2.5 years before (*bottom*; preseismic period). Twenty open circles with five nodes represent observation points of DONET 1 as shown in Figs. 6 and 7. This figure is modified from Ariyoshi and Kaneda [4]

Figure 8 shows examples of simulation results around Tonankai region, which suggests that monitoring the shallower part of slow earthquakes may be effective on the ground that it is more sensitive to the preseismic change of the megathrust earthquake because of free surface condition. In order to detect the preseismic slip of the next Tonankai earthquake in the near future, DONET would play an important role in monitoring shallower part of slow earthquake migration from the view of shortening recurrence interval and increasing migration speed.

We must develop and expand DONET not only in nationwide (DONET 2, 3 to be installed) but also worldwide of major subduction zones in order to mitigate the catastrophic disasters due to coupled megathrust earthquakes.

Acknowledgements The authors would like to deeply appreciate Professor H. Kobayashi for his inviting me to the Workshop on Sustained Simulation Performance 2012. The authors also thank DONET members and Tohoku University researchers. This study was partly supported by supercomputing resources at Cyberscience Center in Tohoku University and at Earth Simulator in JAMSTEC and by Grant-in-Aid (KAKENHI) for Young Scientists 23710212 and for Scientific Research on innovative Areas 20190449.

References

1. Ariyoshi, K., T. Matsuzawa, Y. Yabe, N. Kato, R. Hino, A. Hasegawa, and Y. Kaneda, Character of slip and stress due to interaction between fault segments along the dip direction of a subduction zone, *J. Geodyn.*, 48, 55–67, doi:10.1016/j.jog.2009.06.001, (2009).
2. Ariyoshi, K., T. Matsuzawa, Y. Yabe, N. Kato, R. Hino, and A. Hasegawa, Consideration on the 2011 off the Pacific Coast of Tohoku Earthquake and the 2004 Sumatra Earthquake, *JAMSTEC Rep. Res. Dev.*, 13, 17–33 (2011).
3. Ariyoshi, K. and Y. Kaneda, Characteristics of Interaction between Interplate Earthquakes from the view of Multi-scale Simulations, Nova Publication, in press (2012).
4. Ariyoshi, K. and Y. Kaneda, Frictional Characteristics in Deeper Part of Seismogenic Transition Zones on a Subduction Plate Boundary, *Earthquake Research and Analysis - Seismology, Seismotectonic and Earthquake Geology*, Sebastiano D'Amico (Ed.), ISBN: 978-953-307-991-2, InTech, pp. 402, 105–124, doi:10.5772/28884, (2012).
5. Bilham, R., R. Engdahl, N. Feldl, and S.P. Satyabala, Partial and complete rupture of the Indo-Andaman plate boundary 1847–2004, *Seismo. Res. Lett.*, 76(3), 299–311 (2005).
6. Briggs, R. W., K. Sieh, A. J. Meltzner, D. Natawidjaja, J. Galetzka, B. Suwargadi, Y. Hsu, M. Simons, N. Hananto, I. Suprihanto, D. Prayudi, J. Avouac, L. Prawirodirdjo, and Y. Bock, Deformation and slip along the Sunda megathrust in the great 2005, Nias–Simeulue earthquake, *Science*, 311, 1897–1901 (2006).
7. Coffin, M.F., L.M. Gahagan, and L.A. Lawver, Present-day Plate Boundary Digital Data Compilation, University of Texas Institute for Geophysics Technical Report, 174, 5 (1998).
8. Dieterich, J.H., Modeling of rock friction: 1. Experimental results and constitutive equations, *J. Geophys. Res.*, 84, 2161–2168 (1979).
9. Fujii, Y. and M. Matsu'ura, Regional Difference in Scaling Laws for Large Earthquakes and its Tectonic Implication, *Pure Appl. Geophys.*, 157, 2283–2302 (2000).
10. Furumura, T., K. Imai, and T. Maeda, A revised tsunami source model for the 1707 Hoei earthquake and simulation of tsunami inundation of Ryuujin Lake, Kyushu, Japan, *J. Geophys. Res.*, 116, B02308, doi:10.1029/2010JB007918, (2011).

11. Geospatial Information Authority of Japan, The 2011 off the Pacific coast of Tohoku Earthquake: Postseismic Slip Distribution Model (Preliminary), <http://www.gsi.go.jp/cais/topic110315.2-index-e.html>, (2011)
12. Hsu, Y., M. Simons, J. Avouac, J. Galetzka, K. Sieh, M. Chlieh, D. Natawidjaja, L. Prawirodirdjo, and Y. Bock, Frictional afterslip following the 2005 Nias–Simeulue earthquake, Sumatra, *Science*, 312, 1921–1926 (2006).
13. Japan Meteorological Agency, The 2011 off the Pacific coast of Tohoku Earthquake 15 th report (in Japanese), <http://www.jma.go.jp/jma/press/1103/13b/kaisetsu201103131255.pdf>, (2011).
14. Kanamori, H. and D.L. Anderson, Theoretical basis of some empirical relations in seismology, *Bull. Seism. Soc. Am.*, 65, 1073–1095 (1975).
15. Kato, N., Numerical simulation of recurrence of asperity rupture in the Sanriku region, northeastern Japan, *J. Geophys. Res.*, 113, B06302, doi:10.1029/2007JB005515, (2008).
16. Kido, M., H. Fujimoto, S. Miura, Y. Osada, K. Tsuka, and T. Tabei, Seafloor displacement at Kumano-nada caused by the 2004 off Kii Peninsula earthquakes, detected through repeated GPS/Acoustic surveys, *Earth Planets Space*, 58, 911–915 (2006).
17. Konca, A.O., J. Avouac, A. Sladen, A.J. Meltzner, K. Sieh, P. Fang, Z. Li, J. Galetzka, J. Genrich, M. Chlieh, D.H. Natawidjaja, Y. Bock, E.J. Fielding, C. Ji, and D.V. Helmberger, Partial rupture of a locked patch of the Sumatra megathrust during the 2007 earthquake sequence, *Nature*, 456, 631–635 (2008).
18. Kondo, H., Y. Awata, . Emre, A. Doan, S. zalp, F. Tokay, C. Yildirim, T. Yoshioka, and K. Okumura, Slip Distribution, Fault Geometry, and Fault Segmentation of the 1944 Bolu-Gerede Earthquake Rupture, North Anatolian Fault, Turkey, *Bull. Seism. Soc. Am.*, 95, 1234–1249 (2005).
19. Lay, T., H. Kanamori, C.J. Ammon, M. Nettles, S.N. Ward, R.C. Aster, S.L. Beck, S.L. Bilek, M.R. Brudzinski, R. Butler, H.R. DeShon, G. Ekstrm, K. Satake, and S. Sipkin, The great Sumatra-Andaman earthquake of 26 December 2004, *Science*, 308, 1127–1133, doi:10.1126/science.1112250, (2005).
20. Mogi, K., Two grave issues concerning the expected Tokai Earthquake, *Earth Planets Space*, 56, li–lxvi (2004).
21. Nagai, R., M. Kikuchi, and Y. Yamanaka, Comparative study on the source processes of recent large earthquakes in Sanriku-oki region: The 1968 Tokachi-oki earthquake and the 1994 Sanriku-oki earthquake, *J. Seismol. Soc. Jpn.*, 54, 267–280, in Japanese, (2001).
22. National Geophysical Data Center, Global Significant Earthquake Database, <http://www.ngdc.noaa.gov/hazard/earthqk.shtml>, (2011).
23. Okada, Y., Internal deformation due to shear and tensile faults in a halfspace, *Bull. Seism. Soc. Am.*, 82, 1018–1040 (1992).
24. Peter, B., An updated digital model of plate boundaries: *Geochemistry, Geophysics, Geosystems*, 4(3), 1027, doi:10.1029/2001GC000252, (2003).
25. Press, W. H., B. P. Flannery, S. A. Teukolsky, and W. T. Vetterling, *Numerical Recipes*, 2nd ed., Cambridge Univ. Press, New York (1992).
26. Rani, S., Singh, S.J., Static deformation of a uniform half-space to a long dip-slip fault, *Geophys. J. Int.* 109, 469–476 (1992).
27. Rice, J.R., Spatio-temporal complexity of slip on a fault, *J. Geophys. Res.*, 98, 9885–9907 (1993).
28. Romanowicz, B., Strike-slip earthquakes on quasi-vertical transcurrent faults: inferences for general scaling relations, *Geophys. Res. Lett.*, 19, 481–484 (1992).
29. Ruina, A., Slip instability and state variable friction laws, *J. Geophys. Res.*, 88, 10,359–10,370 (1983).
30. Sato, H., Some precursors prior to recent great earthquakes along the Nankai trough, *J. Phys. Earth*, 25, S115–S121 (Suppl.) (1977).
31. Savage, J.C., A dislocation model of strain accumulation and release at a subduction zone, *J. Geophys. Res.*, 88, 4984–4996 (1983).
32. Scholz, C.H., Scaling laws for large earthquakes; consequences for physical models, *Bull. Seism. Soc. Am.* 72, 1–14 (1982).

33. Sieh, K., The repetition of large-earthquake ruptures, *Proc. Natl. Acad. Sci.*, 93, 3764–3771 (1996).
34. The Headquarters for Earthquake Research Promotion, Long-term Evaluation of seismic activity off Boso to Sanriku (in Japanese), http://www.jishin.go.jp/main/chousa/kaikou.pdf/sanriku_boso.pdf, (2002)
35. The Headquarters for Earthquake Research Promotion, Long-term Evaluation of occurrence potentials of subduction-zone earthquakes around Hyuga-nada and Nansei island (in Japanese), http://www.jishin.go.jp/main/chousa/04feb_hyuganada/index.html, (2004)
36. Uchida, N., A. Hasegawa, T. Matsuzawa, and T. Igarashi, Pre- and post-seismic slow slip on the plate boundary off Sanriku, NE Japan associated with three interplate earthquakes as estimated from small repeating earthquake data, *Tectonophysics*, 385, 1–15 (2004).
37. Wiseman, K. and R. Bruggmann, Stress and Seismicity Changes on the Sunda Megathrust Preceding the 2007 Mw 8.4 Earthquake, *Bull. Seism. Soc. Am.*, 101(1), 313–326 (2011).
38. Yamanaka, Y., Kikuchi, M., Asperity map along the subduction zone in northeastern Japan inferred from regional seismic data, *J. Geophys. Res.* 109, doi:10.1029/2003JB002683, (2004).